JOURNAL OF APPLIED ELECTROCHEMISTRY 23 (1993) 1273–1279

# An electrochemical model for reduction of $MnO_2$ with $Fe^{2+}$ ions

M. BAYRAMOĞLU, T. TEKIN

*Department of Chemical Engineering, University of Atatürk, Erzurum, Turkey*

Received 26 May 1992; revised 29 April 1993

The reduction kinetics of $MnO_2$ by $Fe^{2+}$ ions in acidic solution have been studied. The effects of stirring rate, particle size, temperature, $Fe^{2+}$ and $H^+$ concentrations have been investigated. Diffusional resistances are negligible above 900 r.p.m. and the rate is controlled by electrochemical reaction. A mixed-potential model developed to describe metallic corrosion has been used in combination with the shrinking core model to explain the reaction kinetics. The overall reaction has been written in terms of cathodic and anodic half-cell reactions. The Tafel equation has been used as a starting point to derive a rate equation. A value of 0.5 has been obtained for charge transfer coefficients, which implies the existence of symmetrical charge barriers. The kinetics of the cathodic reduction reaction are first order with respect to the proton concentration.

**Nomenclature**

| | |
|---|---|
| $D$ | diffusion coefficient ($cm^2\,s^{-1}$) |
| $D_i$ | impeller diameter (cm) |
| $D_T$ | reactor diameter (cm) |
| $d_0$ | initial particle diameter ($\mu m$) |
| $E$ | e.m.f. between platinum and saturated calomel electrode (V) |
| $F$ | Faraday constant. |
| $e$ | electrode potential (V) |
| $e_j$ | liquid–junction potential (V) |
| $k_a$ | rate constant of anodic half-cell reaction |
| $k_c$ | rate constant of cathodic half-cell reaction |
| $k_l$ | Mass transfer coefficient ($cm\,s^{-1}$) |
| $m_0$ | amount of $MnO_2$ charged in the reactor (g) |
| $M$ | Molecular weight of $MnO_2$ |
| $N$ | Stirring speed (r.p.m.) |
| $Re_s$ | Reynolds number for stirring ($ND_i^2/\nu$) |
| $Re_p$ | Reynolds number for particle ($d^{4/3}\epsilon^{1/3}/\nu$) |
| $Sc$ | Schmidt number ($\nu/D$) |
| $Sh$ | Sherwood number ($k_l d/D$) |
| $V$ | Reaction volume ($dm^3$) |
| $X$ | Conversion factor |

*Greek letters*

| | |
|---|---|
| $\sigma_i$ | stoichiometric coefficient of reactant $i$ in Equation 1 |
| $\epsilon$ | stirring energy per unit volume |
| $\nu$ | kinematic viscosity ($cm^2\,s^{-1}$) |
| $\tau$ | time required for complete conversion (min) |

## 1. Introduction

Leaching with pickle liquor is an economical method to beneficiate low-grade oxidized manganese ores [1, 2]. This method is based on the reduction of higher oxides of manganese with $Fe^{2+}$ ions:

$$MnO_2 + 2Fe^{2+} + 4H^+ \rightarrow Mn^{2+} + 2Fe^{3+} + 2H_2O \quad (1)$$

The kinetics of this reaction have been investigated by various authors. It was suggested that with pure $\beta$-$MnO_2$ the reaction proceeded on active sites and was controlled by the diffusion of $Fe^{2+}$ ions [3, 4]. The reaction rate is constant up to 60% conversion, despite a surface area decrease of about 50% and then, due to breaking up of the particles, the reaction is governed by first order kinetics. The rotating disc electrode was used to investigate the kinetics of this reaction; for pyrolusite ore [5], diffusion controlled first order reaction kinetics were reported, with an activation energy of $12.2\,kJ\,mol^{-1}$, the rate constant being proportional to $Re^{0.43}.[H_2SO_4]^{0.25}$, where $Re$ is Reynolds number calculated using angular velocity of the disc. For electrolytic $MnO_2$ [6], a mechanism was proposed according to which the slow stage was the formation of an intermediate solid product, MnOOH. On the other hand, Majima *et al.* proposed an electrochemical mechanism [7]. These authors reported a rate independent of $H_2SO_4$ concentration, an order of 0.85 with respect to $Fe^{2+}$ and an activation energy of $14\,kJ\,mol^{-1}$. In the extraction of manganese from low-grade oxidized ores using $FeSO_4$, the nucleation of reaction products on active sites was proposed as the rate determining step and the random nucleation equation, $-\log(1 - X) = kt^{0.5}$, was used to explain the kinetic data [1].

Despite these investigations, the kinetics and mechanism of Reaction 1 are not clear. These differences between results may be due to poorly controlled experimental hydrodynamic conditions. The purpose of this paper is to explore the intrinsic kinetics of this reaction and to establish a model consistent with the kinetic data.

0021-891X 

## 2. Experimental details

Using the thermal decomposition of analytical grade $Mn(NO_3)_2$, $\beta$-$MnO_2$ was prepared [8]. Chemical analysis showed that the atomic ratio (O/Mn) was equal to 2.

Experiments were conducted in a 0.6 $dm^3$, jacketed, cylindrical glass reactor with diameter of 10 cm. It was equipped with four baffles equally spaced, 0.1 $D_T$ in width. The flanged cover of the reactor consisted of sockets for a stirrer, a thermometer, a reflux condenser, inert gas entrance, a platinum electrode and a salt bridge. A four bladed turbine impeller with $D_i = D_T/2$ was located at a height of $D_T/4$ from the bottom. It was driven by a 100 W motor and the stirring rate was controlled to $\mp 1$ r.p.m. The reactor temperature was maintained within $\mp 0.1$°C. Helium gas was passed through the reactor to prevent the oxidation of $Fe^{2+}$ by air. The volume of solution in the reactor was 0.4 $dm^3$. The maximum concentration change of reactants, $H^+$ and $Fe^{2+}$, was limited to 5% by adjusting the amount of $MnO_2$ (10–100 mg).

The reaction was monitored by measuring the e.m.f. between a saturated calomel electrode and a platinum electrode. For this purpose, a voltmeter with 0.5 mV precision was connected to a plotter of high input impedance (10 MΩ).

The e.m.f. of the cell is:

$$E = e_{Fe^{2+}/Fe^{3+}} - e_{cal} + e_j = E_0 - \frac{RT}{F} \ln\left(\frac{a_{Fe^{2+}}}{a_{Fe^{3+}}}\right) + e_j \tag{2}$$

The composition of the solution remained almost constant during reaction. The ionic strength, ionic activity coefficients and the junction potential were also constant, due to the composition of the solution. Thus, for any conversion, $X$, Equation 2 may be written as

$$E_x = A + \frac{RT}{F} \ln\left[\frac{C_{Fe^{3+}}}{C_{Fe^{2+}}}\right]_x \tag{3}$$

The maximum change in $Fe^{2+}$ concentration was limited to 5%. Thus, it may be assumed that $(C_{Fe^{2+}})_0 \simeq (C_{Fe^{2+}})_x \simeq (C_{Fe^{2+}})_1$. If Equation 3 is written for $X = 0$ and $X = 1$ and is rearranged, the following expression is obtained:

$$\frac{(C_{Fe^{3+}})_x - (C_{Fe^{3+}})_0}{(C_{Fe^{3+}})_1 - (C_{Fe^{3+}})_0} = \frac{\exp\left(\dfrac{E_x - E_0}{RT/F}\right) - 1}{\exp\left(\dfrac{E_1 - E_0}{RT/F}\right) - 1} \tag{4}$$

The left hand side of Equation 4 is the conversion, $X$:

$$X = \frac{\exp\left(\dfrac{E_x - E_0}{RT/F}\right) - 1}{\exp\left(\dfrac{E_1 - E_0}{RT/F}\right) - 1} \tag{5}$$

Equation 5 was tested as follows: known weights of $MnO_2$ were added sequentially to 0.4 $dm^3$ of $Fe^{2+}$ solution and when the reaction was complete, redox potentials were noted. Conversions were calculated both by Equation 5 and from sample weights. These two conversion values were tested by linear regression analysis with zero intercept. With 12 data points, a slope equal to 1 was obtained with a correlation coefficient of 0.9989.

## 3. Results and discussion

### 3.1. *Reaction kinetics*

A minimum stirring rate, $N_c$, is required for complete dispersion of particles in a liquid medium. Below this critical speed, the total surface area of particles is not available for reaction and the rate of mass transfer also depends strongly on stirring rate. This critical speed, calculated according to the Zwietering correlation [9], is approximately 630 r.p.m. for the coarsest particles (230 $\mu$m) used in this study. Experiments were carried out for stirring rates of 650, 800, 900 and 1000 r.p.m. The results are given in Fig. 1. Above 900 r.p.m., the reaction rate is not influenced by stirring rate. Consequently, diffusion is not rate limiting. Meanwhile, to confirm this conclusion, further analysis was performed. In the literature, various correlations exist for calculating mass transfer coefficients above the critical stirring speed [10–12], which have the general dimensionless form:

$$Sh = 2 + a\, Re_p^{\gamma}\, Sc^{\beta} \tag{6}$$

where $Re_p$ is given by:

$$Re_p = \frac{d^{4/3}\epsilon^{1/3}}{\nu} = \frac{d_0^{4/3}(1-X)^{4/9}\epsilon^{1/3}}{\nu} \tag{7}$$

If it is assumed that the reaction is controlled by diffusion of the reactant $i$:

$$r_i = \sigma_i \frac{m_0}{M}(dX/dt) = Sk_1C_i \tag{8}$$

where $S$, the total surface area of the spherical particles, is given by

$$S = \frac{6m_0(1-X)}{\rho d_0(1-X)^{1/3}} \tag{9}$$

The stirring is fully turbulent at 900 r.p.m., as the stirring Reynolds number, $Re_s$, is much greater than $1 \times 10^4$:

$$Re_s = \frac{ND_i^2}{\nu} = 4 \times 10^5 \tag{10}$$

So, $k_1$ is obtained from Equation 6 as follows:

$$k_1 \simeq \frac{Da\, Re_p^{\gamma}\, Sc^{\beta}}{d} = \frac{Da\,\epsilon^{\gamma/3}\, Sc^{\beta}(1-X)^{(4\gamma-3)/9}}{\nu^{\gamma} d_0^{(3-4\gamma)/3}} \tag{11}$$

By combining Equations 6–9 and 11 and integrating the resulting differential equation, the following is obtained:

$$t = \tau[1 - (1-X)^{(6-4\gamma)/9}] \tag{12}$$

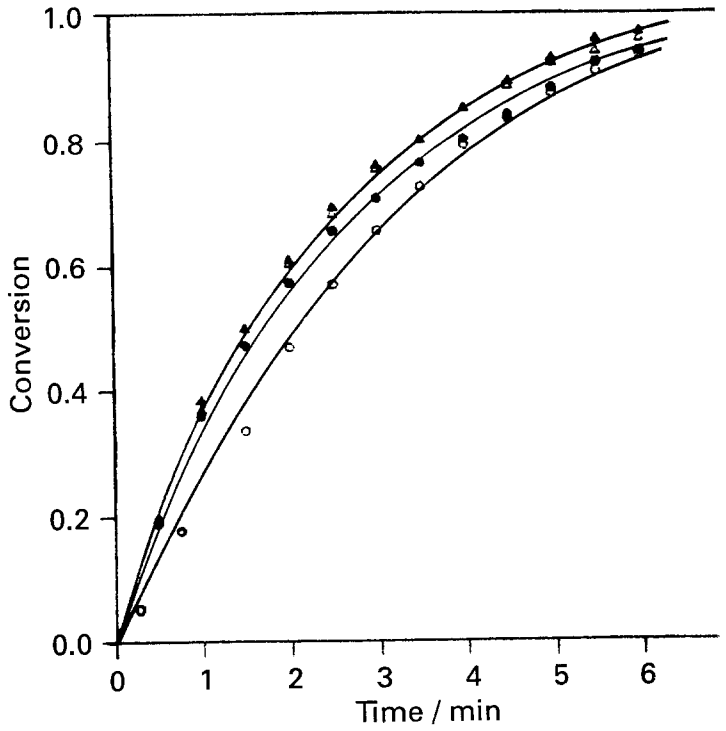


Fig. 1. Effect of stirring rate on conversion. Conditions: $T = 50\,^{\circ}C$, $C_{Fe^{2+}} = 0.2\,M$, $C_{H^+} = 0.1\,M$, $d_0 = 231\,\mu m$. Key: (○) 600, (●) 800, (△) 900 and (▲) 1000 r.p.m.

If the correlation of Batchelor is applied ($\gamma = 0.5$) [11], Equation 12 gives

$$t = \tau[1 - (1 - X)^{4/9}] \tag{13}$$

where

$$\tau = \frac{0.543\sigma_i \rho d_0^{4/3} \nu^{0.5}}{MD\,\epsilon^{1/6} Sc^{1/3} C_i} \tag{14}$$

On the other hand, for a surface reaction limited case, if the shrinking core model of no product layer formation is accepted, the following rate equation is valid [13]:

$$t = \tau[1 - (1 - X)^{1/3}] \tag{15a}$$

where

$$\tau = \frac{\rho d_0}{f(k, C_{Fe^{2+}}, C_{H^+})} \tag{15b}$$

When Equations 13 and 15a were applied to 12 experimental results obtained at 900 r.p.m., linear regression analysis gave correlation coefficients of 0.966 for Equation 13 and 0.9911 for Equation 15a, respectively. A Williams and Kloot statistical test [14] also showed that Equation 15a was the correct model. To further assess the effect of particle size on reaction rate, experiments were conducted with five different particles sizes; e.g., 231, 165, 115, 69 and 49 $\mu$m. The plots of $[1 - (1 - X)^{1/3}]$ against time are shown in Fig. 2(a). The dependence of $\tau$ values on initial partical size is also shown in Fig. 2(b). As predicted by the model, Equation 15a, $\tau$ values were found to be directly proportional to $d_0$.

To clarify the functional dependence of rate equation on reactant concentrations, 16 experiments were conducted in the ranges 0.01 – 0.25 M for $Fe^{2+}$ and 0.01 – 0.1 M for $H_2SO_4$. The true $H^+$ concentrations in $FeSO_4$–$H_2SO_4$ solutions must be known. As indicated by Crundwell [15], the following ionic equilibria exist:

$$H^+ + SO_4^{2-} \xrightarrow{kern - 25} HSO_4^- \tag{16}$$

$$Fe^{2+} + SO_4^{2-} \rightleftharpoons FeSO_4^0 \tag{17}$$

$$Fe^{2+} + SO_4^{2-} + H^+ \rightleftharpoons FeHSO_4^+ \tag{18}$$

By using stability constants given by Crundwell [15] and Pitzer [16] as shown in Table 1, true $H^+$ concentrations were numerically calculated.

For the function $f(C_{Fe^{2+}}, C_{H^+})$, the general form $(C_{Fe^{2+}})^c.(C_{H^+})^d$ was tried and linear regression analysis was executed between $\log(\tau)$ and $\log(C_{H^+})$, $\log(C_{Fe^{2+}})$. With 16 data points, the correlation coefficient was found to be 0.974. The values of $c$ and $d$, with their standard deviation and 99 percentage confidence levels are as follows:

$$c = 0.581 \quad S_c = 0.0368 \quad 0.485 < c < 0.677$$

$$d = 0.545 \quad S_d = 0.0565 \quad 0.398 < d < 0.692$$

These confidence levels suggested a value of 0.5 for both $c$ and $d$. Thus, it was decided to regress $\tau$ on $(C_{Fe^{2+}})^{0.5}.(C_{H^+})^{0.5}$ values. The result is shown in Fig. 3.

Finally, experiments were conducted to calculate the apparent activation energy of the reaction in the temperature range 308 to 328 K. Figure 4 shows $[1 - (1 - X)^{1/3}]$ against time for various temperatures. The Arrhenius plot is given in Fig. 5. The

*Table 1. Equilibrium constants*

| *Reaction* | *Equilibrium constants* |
|---|---|
| $H^+ + SO_4^{2-} \rightleftharpoons HSO_4^-$ | $\exp(-14.021 + 2825.2/T)$ |
| $Fe^{2+} + SO_4^{2-} \rightleftharpoons FeSO_4^0$ | $\exp(7.688 - 776.8/T)$ |
| $Fe^{2+} + SO_4^{2-} + H^+ \rightleftharpoons FeHSO_4^+$ | $\exp(30.690 - 7290.4/T)$ |

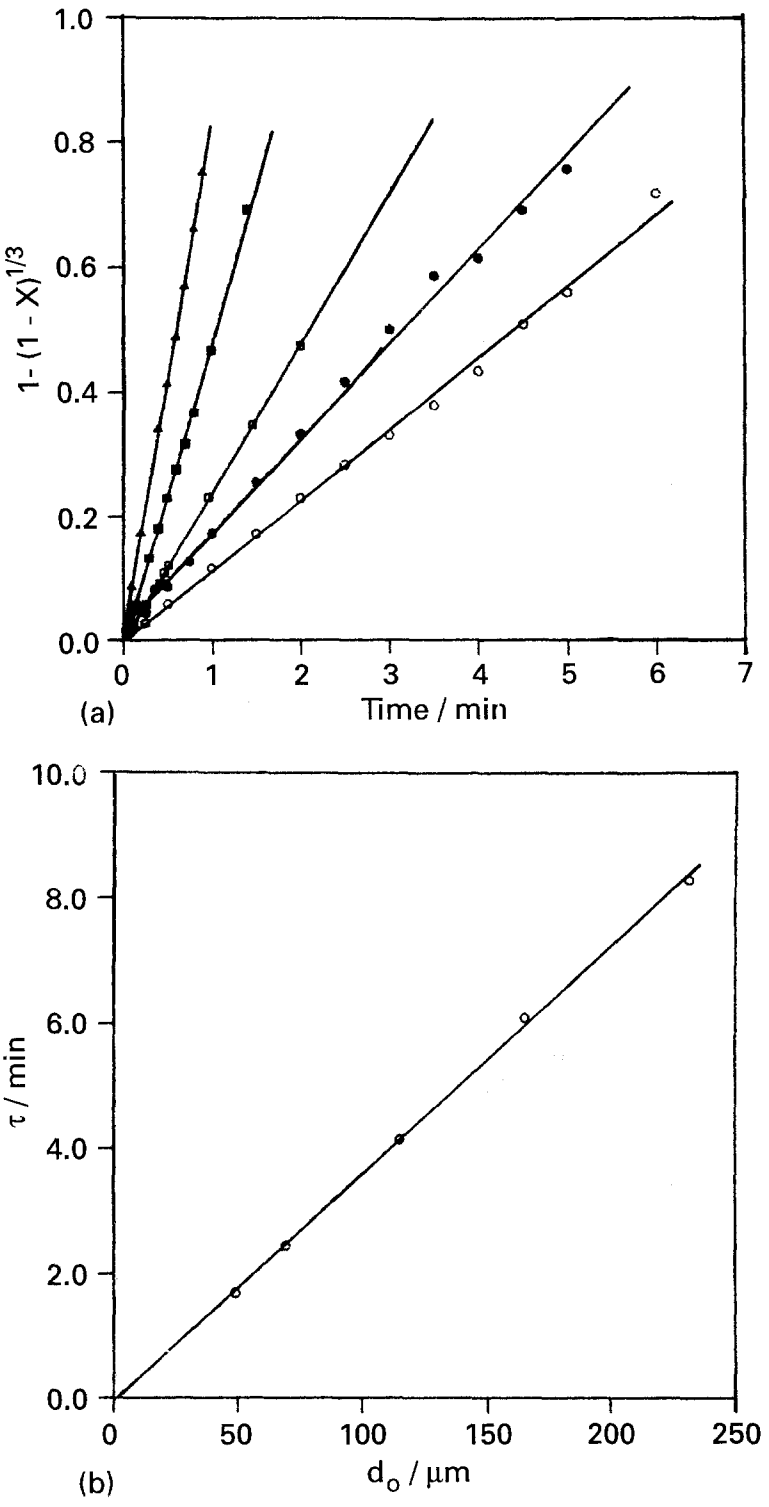


Fig. 2. (a) Plot of $[1-(1-X)^{1/3}]$ against time for different particle sizes. Key: (○) 231, (●) 165, (□) 115, (■) 69 and (△) 49 $\mu$m. (b) Plot of time against initial particle size. Conditions: $T = 50\,^{\circ}C$, $C_{Fe^{2+}} = 0.1\,M$, $C_{H^+} = 0.1\,M$, $N = 900$ r.p.m.

apparent activation energy, $E_a$, obtained from the slope is $27.6\,kJ\,mol^{-1}$. Thus, the following relation was obtained experimentally for $\tau$:

$$\tau = \frac{\rho d_0}{8.7 \times 10^6\ M \exp(-27600/RT)(C_{Fe^{2+}})^{0.5}(C_{H^+})^{0.5}} \quad (19)$$

### 3.2. *Electrochemical model*

It is well known that the rate determining step in many reductive or oxidative dissolution processes is an electron transfer step. So, the mixed-potential model developed to describe metallic corrosion processes has been applied in combination with shrinking-core model to the dissolution kinetics of some semiconductors, e.g. ZnS, in $Fe^{3+}$ solution [15, 17]. Manganese dioxide is an n-type semiconductor, its rest potential corresponds to the equilibrium electrode potential, which depends on the solution composition according to the Nernst equation [18]. On the other hand, if it is assumed that the potential across the solid side of the interface is approximately constant so that the applied potential appears only across the Helmoltz layer, the rate of electron transfer may be

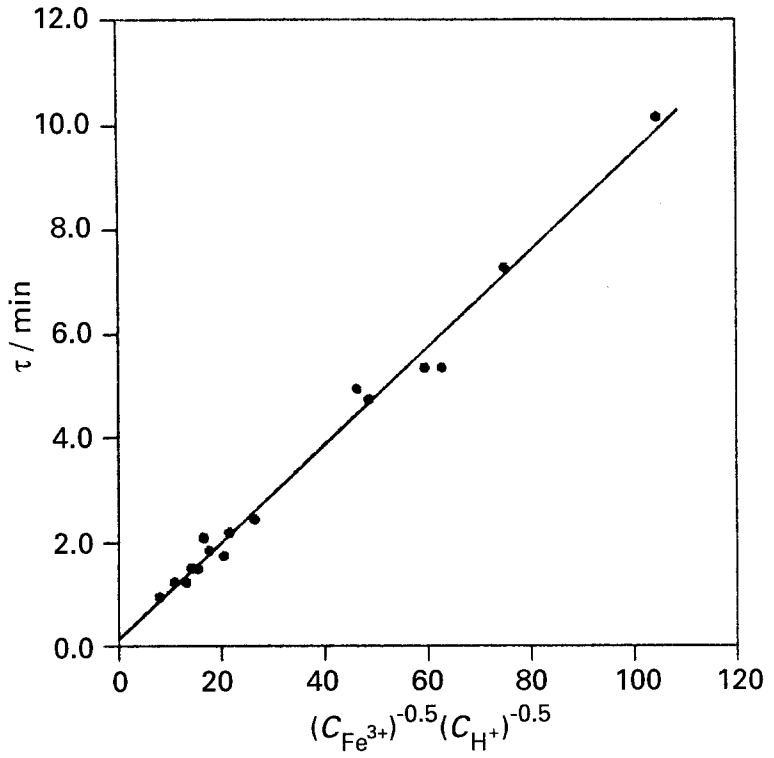


Fig. 3. Plot of $\tau$ against $(C_{Fe^{2+}})^{-0.5} \times (C_{H^+})^{-0.5}$. Conditions: $T = 50°C$, $N = 900$ r.p.m., $d_0 = 49\,\mu m$.

described by the Tafel equation, which relates the current density to the potential across the Helmholtz layer.

The equilibrium constant of Reaction 1 at 298 K is approximately $2 \times 10^{15}$. Thus, in acidic solution, Reaction 1 is almost irreversible. The cathodic and anodic half-cell reactions are written separately:

$$MnO_2 + 4H^+ + 2e^- \rightarrow Mn^{2+} + 2H_2O \quad (20)$$

$$Fe^{2+} \rightarrow Fe^{3+} + e^- \quad (21)$$

As the effects of back reactions and mass transport are negligible, the net anodic and cathodic current densities are as follows, according to Tafel equations,

$$i_c = -n_c F k_c C^m_{H^+} \exp[-(1 - \alpha_c) z_c FE/RT] \quad (22)$$

$$i_a = n_a F k_a C_{Fe^{2+}} \exp[\alpha_a z_a FE/RT] \quad (23)$$

where $n_c = 2$, $n_a = 1$, $\alpha_a$ and $\alpha_c$ represent the symmetry of the activation barrier for the half-cell charge transfer reactions, respectively. Since no net current flows during the dissolution of a particle, $i_c + i_a = 0$.

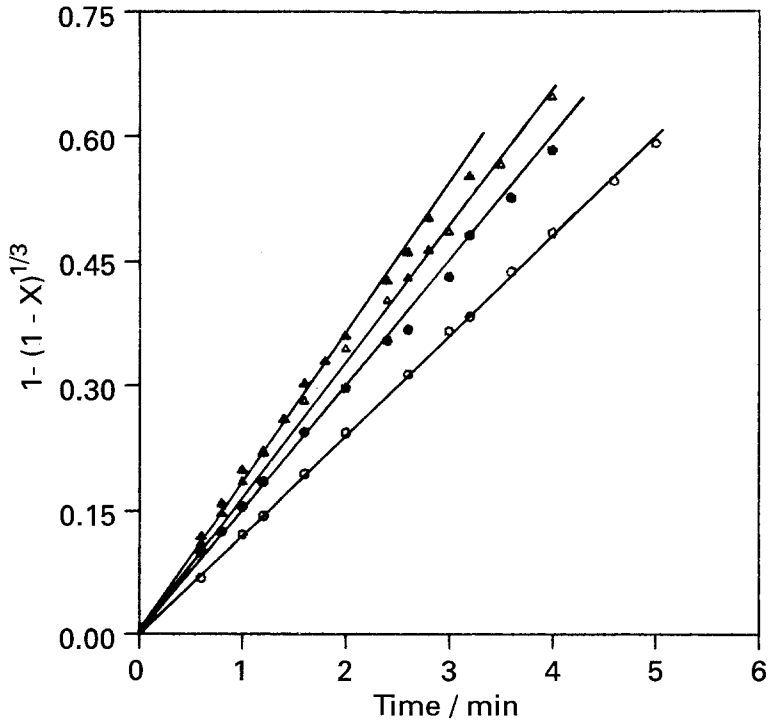


Fig. 4. Plot of $[1 - (1 - X)^{1/3}]$ against time at different temperatures. Conditions: $C_{Fe^{2+}} = 0.02$ M, $C_{H^+} = 0.04$ M, $N = 900$ r.p.m., $d_0 = 49\,\mu m$. Key: (○) 308, (●) 318, (△) 323 and (▲) 328 K.

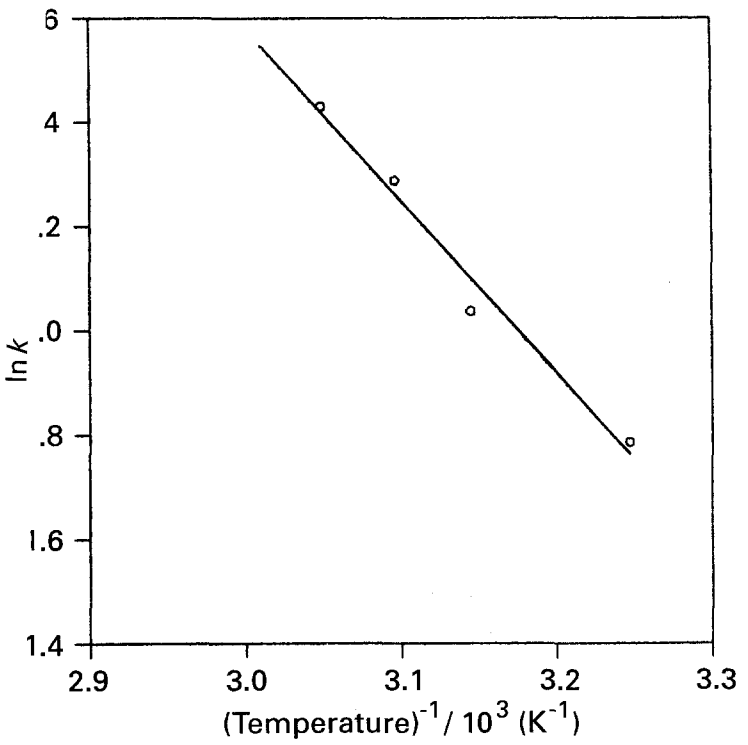


Fig. 5. Arrhenius plot of log($k$) against (temperature)$^{-1}$. ($k = (C_{Fe^{2+}})^{0.5}.(C_{H^+})^{0.5}/\tau$).

The exchange current density, $i_0$, at the mixed potential $E_m$, is given as

$$i_0 = 2Fk_cC_{H^+}^m \exp[-(1-\alpha_c)z_cFE_m/RT] = Fk_aC_{Fe^{2+}} \exp[\alpha_\alpha z_aFE_m/RT] \quad (24)$$

let

$$\lambda = \frac{\alpha_a z_a}{\alpha_a z_a + (1-\alpha_c)z_c} \quad (25)$$

So

$$i_0 = Fk_a^{1-\lambda}2^\lambda k_c^\lambda (C_{Fe^{2+}})^{1-\lambda}(C_{H^+}^m)^\lambda \quad (26)$$

On the other hand, the overall reaction rate can be expressed as:

$$\frac{m_0}{M}\left(\frac{dX}{dt}\right) = \frac{fSi_0}{2F} \quad (27)$$

where $f$ is the ratio of the area of active sites to total surface area of a particle, and $S$ is given by Equation 9. From Equations 9, 24 and 25, the following is obtained after integration:

$$\tau = \frac{\rho d_0}{Mf2^\lambda k_a^{1-\lambda}k_c^\lambda (C_{Fe^{2+}})^{1-\lambda}(C_{H^+}^m)^\lambda} \quad (28)$$

When orders of $C_{Fe^{2+}}$ in Equations 19 and 28 are compared, it is deduced that $\lambda = 0.5$ and, from the orders of $C_{H^+}$, $m = 1$. Thus, it is concluded that Reaction 20 is first order with respect to $H^+$ concentration. On the other hand, from Equation 25, $\alpha_a z_a = (1-\alpha_c)z_c$ and, as $Fe^{2+}$ ion is a single electron transfer agent, $z_a = z_c = 1$, so, $\alpha_a + \alpha_c = 1$. The most probable value for the charge transfer coefficients, $\alpha_a$ and $\alpha_c$, is 0.5, which means that the charge barriers are symmetrical. Finally, for the anodic and cathodic rate constants, $k_a$ and $k_c$, the following relation is obtained:

$$f(k_ak_c)^{0.5} = 6.2 \times 10^6 \exp(-27600/RT) \quad (29)$$

## 4. Conclusion

The kinetics of the reaction of $\beta$-$MnO_2$ particles with $Fe^{2+}$ ions in $H_2SO_4$ solution were investigated. Above 900 r.p.m., diffusional effects are negligible and the rate is controlled by an electrochemical surface reaction which can be described by a combination of mixed potential-shrinking core models. Single electron transfer possibly occurs with symmetrical activation barriers. The hydrated $Fe^{2+}$ and other sulphate complexes are also electro active species. The final rate equation is given by

$$t = \frac{\rho d_0}{8.7 \times 10^9 \text{ M} \exp(-27600/RT)(C_{Fe^{2+}})^{0.5}(C_{H^+})^{0.5}} \times [1-(1-X)^{1/3}] \quad (30)$$

where $t$ is expressed in min.

## References

[1] S. C. Das, D. K. Sahoo and P. K. Rao, *Hydrometallurgy* **15** (1982) 35.
[2] R. D. Hoak and J. Coull, *Chem. Eng. Progress* **46** (1950) 158.
[3] D. F. A. Koch and A. Walkley, Trabajos Reunion Intern. React. Solidos, 3rd, Madrid, Vol. 1 (1956) p. 453.
[4] G. M. Nesmeyanova and A. I. Vikulov, *Zhurn. Prikl. Khimii* **35** (1962) 989.
[5] R. G. Dundua and G. N. Dobrokhotov, *ibid.* **55** (1982) 1831.
[6] R. I. Agladze and G. D. Shengeliya, *ibid.* **56** (1983) 1765.
[7] H. Majma, Y. Awakura, Y. Sosaki and T. Teranishi, *Nippon Kogyo Kaishi* **97** (1981) 267.
[8] J. Y. Welsh *US Patent 3 780 158* (1973).
[9] T. N. Zwietering, *Chem. Eng. Sci.* **8** (1958) 244.
[10] P. M. Armenante and J. D. Kirwan, *ibid.* **44** (1989) 2781.
[11] C. K. Batchelor, *J. Fluid Mech.* **98** (1980) 609.

[12] D. M. Levins and J. R. Glastonbury, *Trans. Inst. Chem. Eng.* **50** (1972) 132.
[13] O. Levenspiel, 'Chemical Reaction Engineering', 2nd edn, John Wiley & Sons, New York (1972) p. 369.
[14] D. M. Himmelblau, 'Process Analysis by Statistical Methods', John wiley & Sons, New York (1969) p. 216.
[15] F. K. Crundwell, *Hydrometallurgy* **20** (1987) 227.
[16] K. S. Pitzer, N. R. Roy and F. L. Silvester, *J. Am. Chem. Soc.* **99** (1977) 4930.
[17] B. Verbaan and F. K. Crundwell, *Hydrometallurgy* **16** (1986) 345.
[18] J. D. Miller and R. Y. Wang, *ibid.* **10** (1983) 219.